Available online at http://scik.org
Commun. Math. Biol. Neurosci. 2024, 2024:93
https://doi.org/10.28919/cmbn/8785
ISSN: 2052-2541

THE MATHEMATICAL MODELING AND ANALYSIS OF THE CHOLERA DISEASE MODEL

ISSAM SAHIB[1,*], MOHAMED BAROUDI[1], HICHAM GOURRAM[1], BOUCHAIB KHAJJI[2], ABDERRAHIM LABZAI[2], MOHAMED BELAM[1]

[1]Laboratory LMACS, Sultan Moulay Slimane University, MATIC Research Team: Applied Mathematics and Information and Communication Technologie, Department of Mathematics and Computer Science, Khouribga Polydisciplinary Faculty, Morocco

[2]Laboratory of Analysis Modeling and Simulation, Department of Mathematics and Computer Science, Faculty of Sciences Ben M'sik, Hassan II University of Casablanca, Morocco

Abstract. We are developing a deterministic model for cholera that incorporates immunization campaigns, treatment of infected individuals, and efforts to sanitize water supplies. This model offers precise and valuable insights into specific aspects of cholera control. The basic reproduction number, R_0, derived from the disease-free equilibrium (DFE), serves as a critical metric for assessing disease control efforts. Our stability analysis reveals that the DFE is asymptotically stable both locally and globally when R_0 is less than one. Sensitivity analysis of R_0 underscores the importance of vaccination, treatment, public awareness campaigns, and sanitation in controlling cholera. We explore the local and global stability of both the disease-free and disease-endemic equilibrium by constructing Lyapunov functions and applying the Routh-Hurwitz criteria. Additionally, we perform sensitivity analyses to identify the parameters that significantly impact R_0. Finally, numerical simulations using Matlab are conducted to validate our theoretical findings.

Keywords: mathematical modeling; stability; Lyapunov functions; sensitivity; optimal control.

2020 AMS Subject Classification: 92C60.

*Corresponding author

E-mail address: Sahibissam@gmail.com

Received July 28, 2024

1. INTRODUCTION

Cholera continues to pose a significant global public health challenge, causing tens of thousands of deaths annually worldwide [1]. The transmission rate within communities is affected by various social and environmental factors, with seasonal variations in contact rates contributing to recurrent outbreaks in certain regions [2, 3]. Understanding these dynamics requires an accurate estimation of Vibrio cholerae prevalence in endemic populations and a thorough comprehension of the relationship between bacterial concentration and virulence [2]. Seasonal changes in contact rates are critical in driving the cyclical nature of cholera outbreaks [4].

In 2001, researchers enhanced Capasso's model by incorporating the environmental presence of Vibrio cholerae in water supplies into a basic SIR framework, utilizing a logistic function to account for incidence and saturation effects. Further refinement was made by Hartley et al. (2006), who introduced a hyper-infectious stage in Codeco's model, reflecting the increased transmissibility of recently shed Vibrio cholerae observed in laboratory studies [4].

During cholera outbreaks, interventions should focus on reducing the transmission risk of the highly contagious, transient strain of toxigenic Vibrio cholerae. It is also important to explore whether other prevalent diseases exhibit similarly high transmissibility. Identifying such conditions and integrating them into disease prevention models can enhance the precision and effectiveness of targeted interventions, as expanded upon by Joh et al. (2009) in their extension of Codeco's model [5].

Public awareness campaigns are vital for controlling the spread of infectious diseases. These efforts reduce contact transmission among vulnerable populations, especially in the age of rapid information dissemination via social media and increased international travel. Such initiatives have a significant impact on disease dynamics by lowering transmission rates and improving epidemic management [7, 8, 9].

Numerous studies and mathematical models have explored the relationship between human social behavior and the spread of infectious diseases [10, 11, 12, 13, 14, 15]. Specifically, various models have been developed and analyzed to mitigate cholera's impact and reduce the number of affected individuals [17].

This paper is structured as follows: Section 1 introduces the model formulation and its core properties. Section 2 discusses the derivation and stability analysis of the model's equilibrium points. In Section 3, the global stability of the equilibrium point is analyzed. Section 4 delves into the sensitivity of model parameters. Numerical simulations and their interpretations are presented in Section 5. The paper concludes with a summary of the findings in the final section.

2. A Mathematical Model and Basic Properties

2.1. A Mathematical Model. In the context of cholera, we introduce a continuous dynamics model of the $SICR-B$ type (Susceptible-Infectious-Centers-Recovered-Bacterial), which incorporates bacterial concentration. The total population, $N(t)$, is categorized into four groups: susceptible individuals $S(t)$, infected individuals $I(t)$ who exhibit symptoms, individuals receiving treatment in centers $C(t)$, and recovered individuals $R(t)$. The total population at any given time t is expressed as $N(t) = S(t)+I(t)+C(t)+R(t)$. A graphical representation of this model is provided in Figure 1.

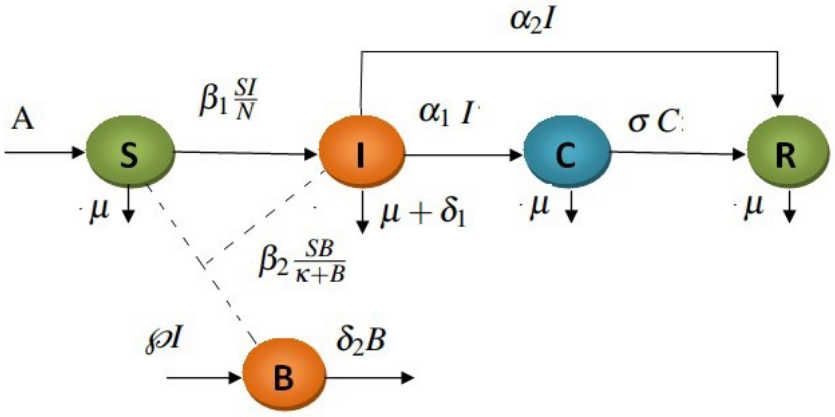

FIGURE 1. The dynamics among the five compartments $SICR-B$ of cholera disease.

$$
(1)\qquad \begin{cases} \frac{dS(t)}{dt} = \mathrm{A} - \mu S - \beta_1 \frac{SI}{N} - \beta_2 \frac{SB}{\kappa+B}; \\ \frac{dI(t)}{dt} = \beta_1 \frac{SI}{N} - I(\mu+\delta_1+\alpha_1+\alpha_2) + \beta_2 \frac{SB}{\kappa+B}; \\ \frac{dC(t)}{dt} = \alpha_1 I - (\sigma+\mu)C; \\ \frac{dR(t)}{dt} = \alpha_2 I + \sigma C - \mu R; \\ \frac{dB(t)}{dt} = \wp I - \delta_2 B; \end{cases}
$$

The initial conditions are defined as $S(0) \geq 0$, $I(0) \geq 0$, $C(0) \geq 0$, $R(0) \geq 0$, and $B(0) \geq 0$. For $t > 0$, the total population $N(t)$ is divided into four categories: susceptible individuals $S(t)$, infectious individuals $I(t)$ who exhibit symptoms, individuals receiving treatment in centers $C(t)$, and recovered individuals $R(t)$.

Additionally, we introduce a class $B(t)$, representing the bacterial concentration at time t. We assume a positive recruitment rate A into the susceptible class $S(t)$ and a positive natural death rate μ for all t. Susceptible individuals can contract cholera at a rate $\beta_2 \frac{B(t)}{\kappa+B(t)}$, where $\beta_2 > 0$ represents the rate of bacterial ingestion from contaminated sources, κ is the half-saturation constant of the bacterial population, and $\frac{B(t)}{\kappa+B(t)}$ reflects the probability of infection upon exposure.

Infected individuals may seek treatment in centers where they are isolated and receive appropriate care at rates α_1 and α_2. Recovery from treatment occurs at a rate σ. The disease-related death rates for treated and untreated infected individuals are δ_1 and μ, respectively.

Each infected individual contributes to an increase in bacterial concentration at a rate $\wp$, while the bacterial concentration decreases due to bacterial mortality at a rate δ_2. These dynamics are captured by the following equations.

2.2. Basic Properties of the model.

2.2.1. ***The Invariance Region.*** To demonstrate that all solutions of system (1) remain positive for all $t > 0$ given positive initial values, we will establish this through the following lemma.

Lemma 1: All admissible solutions $S(t), I(t), C(t), R(t),$, and $B(t)$ of the system (1) are bounded within the region.

$$\Omega = \Omega_N * \Omega_B \tag{2}$$

$$\begin{aligned} &\Omega_N = \left\{ (S,I,C,R) \in \Re_+^4 : S+I+C+R \leq \tfrac{\mathrm{A}}{\mu} \right\} \\ &\textit{and} \\ &\Omega_B = \left\{ B \in \Re_+ : B \leq \tfrac{\wp}{\delta_2} \right\} \end{aligned} \tag{3}$$

Proof. From the equation of the system (1)

$$\frac{dN(t)}{dt} = \mathrm{A} - \mu N(t) - I\delta_1. \tag{4}$$

Implies the following.

$$\frac{dN(t)}{dt} \leq \mathrm{A} - \mu N(t).$$

Therefore, it is clear that

$$N(t) \leq \tfrac{\mathrm{A}}{\mu} + N(0)e^{-\mu t}. \tag{5}$$

Since N(0) is the initial value of the total number of people,

$$\lim_{t\to+\infty} SupN(t) \leq \tfrac{\mathrm{A}}{\mu}. \tag{6}$$

then

$$S(t)+I(t)+C(t)+R(t) \leq \frac{\mathrm{A}}{\mu}.$$

Similarly

$$\frac{dB(t)}{dt} = \wp I - \delta_2 B(t) \leq \wp - \delta_2 B(t).$$

$$B(t) \leq \frac{\wp}{\delta_2} + B(0)e^{-\delta_2 t}.$$

$$\lim_{t\to+\infty} SupB(t) \leq \tfrac{\wp}{\delta_2}. \tag{7}$$

$$B(t) \leq \frac{\wp}{\delta_2}.$$

For the analysis of model (1), we get the region which is given by the set.

$$\begin{aligned} &\Omega_N = \left\{(S,I,C,R) \in \Re_+^4 : S+I+C+R \leq \tfrac{\mathrm{A}}{\mu}\right\} \\ &\textit{and} \\ &\Omega_B = \left\{B \in \Re_+ : B \leq \tfrac{\wp}{\delta_2}\right\}. \end{aligned} \tag{8}$$

Which is a positively invariant set for (1), which is a positively invariant set for (1) Therefore, it is only necessary to consider the dynamics of the system (1) in relation to the set of non-negative solutions Ω

2.2.2. *Positivity of solutions of the model*. .

Theorem 1. If $S(0) \geq 0$, $I(0) \geq 0$, $C(0) \geq 0$, $R(0) \geq 0$, and $B(0) \geq 0$, then the solutions of system equation (1), $S(t), I(t), C(t), R(t)$, and $B(t)$, are positive for all $t > 0$.

Proof: Starting from the first equation of system (1), we obtain

$$\frac{dS(t)}{dt} = \mathrm{A} - M(t)S(t). \tag{9}$$

Given that

$$M(t) = \mu + \beta_1 \frac{I(t)}{N} + \beta_2 \frac{B(t)}{\kappa + B(t)}. \tag{10}$$

We multiply equation (9) by $\exp\left(\int_0^t M(s)\,ds\right)$; thus, we obtain:

$$\frac{dS(t)}{dt} * \exp(\int_0^t M(s)ds) = [\mathrm{A} - M(t) * S(t)] * \exp(\int_0^t M(s)ds). \tag{11}$$

$$\frac{dS(t)}{dt} * \exp(\int_0^t M(s)ds) + M(t) * S(t) * \exp(\int_0^t M(s)ds) = \mathrm{A} * \exp(\int_0^t M(s)ds) \tag{12}$$

Therefore

$$\frac{d}{dt}[S(t) * \exp(\int_0^t M(s)ds] = \mathrm{A} * \exp(\int_0^t M(s)ds) \tag{13}$$

When we take the integral with respect to s from 0 to t, we obtain

$$S(t) * \exp(\int_0^t M(s)ds) - S(0) = \mathrm{A} * \int_0^t (\exp(\int_0^w M(s)ds))dw. \tag{14}$$

Multiplying equation (14) by $\exp\left(-\int_0^t M(s)\,ds\right)$, we obtain:

$$S(t) - S(0) * \exp(-\int_0^t M(s)ds) = \mathrm{A} * \exp(-\int_0^t M(s)ds) * \int_0^t (\exp(\int_0^w M(s)ds))dw. \tag{15}$$

Then:

$$S(t) = S(0) * \exp(-\int_0^t M(s)ds) + \mathrm{A} * \exp(-\int_0^t M(s)ds) * \int_0^t (\exp(\int_0^w M(s)ds))dw \geq 0. \tag{16}$$

Thus, $S(t)$ is a positive solution. Similarly, based on the other equations in system (1), we obtain:

$$I(t) \geq I(0) * \exp(-\int (\mu + \delta_1 + \alpha_1 + \alpha_2 - \beta_1 \frac{S(s)}{N})ds \geq 0. \tag{17}$$

$$C(t) \geq C(0) * \exp(-(\sigma+\mu)t) \geq 0. \tag{18}$$

$$R(t) \geq R(0) * \exp(-(\alpha_2+\mu)t) \geq 0. \tag{19}$$

$$B(t) \geq B(0) * \exp(-\delta_2 t) \geq 0. \tag{20}$$

As a result, the proof is finished since we can see that for all $t \geq 0$, the solutions $S(t)$, $I(t)$, $C(t)$, $R(t)$, and $B(t)$ of the system (1) are positive. Since the variables C and R do not affect the first three equations in system (1), the dynamics of equation system (1) is equal to the dynamics of equation system:

$$\begin{cases} \frac{dS(t)}{dt} = \mathrm{A} - \mu S - \beta_1 \frac{SI}{N} - \beta_2 \frac{SB}{\kappa+B}; \\ \frac{dI(t)}{dt} = \beta_1 \frac{SI}{N} - I(\mu+\delta_1+\alpha_1+\alpha_2) + \beta_2 \frac{SB}{\kappa+B}; \\ \frac{dB(t)}{dt} = \wp I - \delta_2 B; \end{cases} \tag{21}$$

3. Stability Analysis and Sensitivity of the Model

3.1. Points of Equilibrium: This model has two equilibrium points: the disease-free equilibrium, which occurs when cholera is absent, and the epidemic equilibrium, which occurs when cholera is present. These points can be determined by setting the derivatives in the system of equations (21) to zero. In the absence of the virus (where $I = B = 0$), the cholera disease-free equilibrium is given by $E^0_{eq} = \left(\frac{A}{\mu}, 0, 0\right)$. When the disease is present (where $I^* \neq 0$ and $B^* \neq 0$), the cholera epidemic equilibrium is reached, denoted by $E^*_{eq} = (S^*, B^*, I^*)$. Where

$$B^* = \frac{\wp}{\delta_2} I^* \tag{22}$$

$$S^* = \frac{N(\delta_2\kappa + \wp I^*)(\mu+\delta_1+\alpha_1+\alpha_2)}{\beta_1(\delta_2\kappa+\wp I^*)+\beta_2 N\wp} \tag{23}$$

The following results from substituting equations (22) and (23) into system (24)'s first equation:

$$a_1 I^{*2} + a_2 I^* + a_3 = 0. \tag{24}$$

Where

$$a_1 = -(\mu+\delta_2+\alpha_1+\alpha_2)\beta_1\wp$$

$$a_2 = A\beta_2\wp - N(\mu+\delta_2+\alpha_1+\alpha_2)(\mu\wp+\delta_2\kappa\frac{\beta_1}{N}+\beta_2\wp)$$

$$a_3 = (\mu+\delta_2+\alpha_1+\alpha_2)\mu N\delta_2\kappa[R_0-1]$$

$$R_0 = \frac{\mathrm{A}}{\mu(\mu+\delta_1+\alpha_1+\alpha_2)}[\frac{\beta_1}{N}+\frac{\beta_2\wp}{\delta_2\kappa}] \tag{25}$$

The basic reproduction number, or R_0, is the average number of new infections that one infected person in a population of full susceptibility causes. The frequency of an outbreak is indicated by the value of R_0. The next generation matrix method described in [19] can be used to calculate the basic reproduction number.

3.2. Analyzing the local stability. .

Now, we will examine equilibrium behavior and stability. E^0_{eq} and E^*_{eq}, respectively.

3.2.1. ***The condition of a disease-free equilibrium.*** This section explores the local stability of the cholera disease-free equilibrium.

Theorem 2. The equilibrium $E^0_{eq} = \left(\frac{A}{\mu},0,0\right)$ of the system (21), which represents a state free from cholera, is asymptotically stable when $R_0 < 1$ and unstable when $R_0 > 1$.

Proof. At E_{eq}, the Jacobian matrix is provided by

$$J(E_{eq}) = \begin{pmatrix} -\mu-\beta_1\frac{I}{N}-\beta_2\frac{B}{\kappa+B} & -\beta_1\frac{S}{N} & -\beta_2\frac{S(\kappa+B)-SB}{(\kappa+B)^2} \\ \beta_1\frac{I}{N}+\beta_2\frac{B}{\kappa+B} & \beta_1\frac{S}{N}-(\mu+\delta_1)-(\alpha_1+\alpha_2) & \beta_2\frac{S(\kappa+B)-SB}{(\kappa+B)^2} \\ 0 & \wp & -\delta_2 \end{pmatrix} \tag{26}$$

For the disease-free equilibrium, the Jacobian matrix is provided by

$$J(E^0_{eq}) = \begin{pmatrix} -\mu & -\beta_1\frac{\mathrm{A}}{\mu N} & -\beta_2\frac{\mathrm{A}}{\kappa\mu} \\ 0 & \beta_1\frac{\mathrm{A}}{\mu N}-(\mu+\delta_1)-(\alpha_1+\alpha_2) & \beta_2\frac{\mathrm{A}}{\kappa\mu} \\ 0 & \wp & -\delta_2 \end{pmatrix} \tag{27}$$

This matrix's characteristic equation is $det(J(E^0_{eq})-\lambda I_3) = 0$, where I_3 is an order three square identity matrix.

Consequently, we can observe that $J(E^0_{eq})$ has the following characteristic equations $\phi(\lambda)$:

$$\phi(\lambda) = (-\mu-\lambda)[(\beta_1\frac{\mathrm{A}}{\mu N}-(\mu+\delta_1+\alpha_1+\alpha_2)-\lambda)(-\delta_2-\lambda)-\wp\beta_2\frac{\mathrm{A}}{\kappa\mu}] \tag{28}$$

The characteristic equation of $J(E^0_{eq})$ has the following eigenvalues:

Then

$$\lambda_1 = -\mu$$

And

(29)

$$\lambda^2 - \lambda[-\delta_2 + \beta_1 \tfrac{A}{\mu N} - (\mu + \delta_1 + \alpha_1 + \alpha_2)] - \delta_2(\beta_1 \tfrac{A}{\mu N} - (\mu + \delta_1 + \alpha_1 + \alpha_2)) - \wp\beta_2 \tfrac{A}{\kappa\mu} = 0$$

One eigenvalue is obviously negative.The characteristic equation of the submatrix J_1 is now equation (30) where:

(30)
$$J_1 = \begin{pmatrix} \beta_1 \frac{A}{\mu N} - (\mu + \delta_1 + \alpha_1 + \alpha_2) & \beta_2 \frac{A}{\kappa\mu} \\ \wp & -\delta_2 \end{pmatrix}$$

If the trace of $J_1 \prec 0$ and the $det(J_1) \succ 0$ then the eigenvalues are negative

The trace of

(31)
$$tr(J_1) = \beta_1 \tfrac{A}{\mu N} - (\mu + \delta_1 + \alpha_1 + \alpha_2) - \delta_2$$

(32)
$$\begin{aligned} &= (\mu + \delta_1 + \alpha_1 + \alpha_2)[-\beta_1 \tfrac{A}{\mu N(\mu+\delta_1+\alpha_1+\alpha_2)} + 1] - \delta_2 \\ &= (\mu + \delta_1 + \alpha_1 + \alpha_2)[-1 + (R_0 - \beta_2 \tfrac{A\wp}{\delta_2\kappa\mu(\mu+\delta_1+\alpha_1+\alpha_2)})] - \delta_2. \end{aligned}$$

Trace $J_1 \prec 0$ if $R_0 \prec 1$

And

(33)
$$\det(J_1) = -\delta_2\beta_1 \tfrac{A}{\mu N} + \delta_2(\mu + \delta_1 + \alpha_1 + \alpha_2) - \wp\beta_2 \tfrac{A}{\kappa\mu} \succ 0$$

That is

(34)
$$\delta_2(\mu + \delta_1 + \alpha_1 + \alpha_2)[1 - \beta_1 \tfrac{A}{\mu N[(\mu+\delta_1)+(\alpha_1+\alpha_2)]} - \beta_2 \tfrac{A\wp}{\delta_2\kappa\mu[(\mu+\delta_1)+(\alpha_1+\alpha_2)]}] \succ 0$$

$$\delta_2(\mu + \delta_1 + \alpha_1 + \alpha_2)[1 - \frac{A}{\mu(\mu + \delta_1 + \alpha_1 + \alpha_2)}(\frac{\beta_1}{N} + \frac{\beta_2\wp}{\delta_2\kappa})] \succ 0)$$

$$\delta_2(\mu + \delta_1 + \alpha_1 + \alpha_2)[1 - R_0] \succ 0$$

$$1 - R_0 \succ 0$$

if

$$1 \succ R_0$$

Consequently, given that each of the characteristic equation's eigenvalues (29) possess a negative real part, it is demonstrated that E_{eq}^0 has a locally asymptotically stable value.

3.2.2. ***Disease present equilibrium.*** In this section, we analyze the local stability of the disease present equilibrium. We consider $\frac{dS}{dt} = 0$, $\frac{dI}{dt} = 0$ and $\frac{dB}{dt} = 0$.

We have

$$B^* = \frac{\wp}{\delta_2} I^* \tag{35}$$

$$S^* = \frac{N(\delta_2\kappa+\wp I^*)(\mu+\delta_1+\alpha_1+\alpha_2)}{\beta_1(\delta_2\kappa+\wp I^*)+\beta_2 N\wp} \tag{36}$$

From the second equation in the system (21), we have

$$a_1 I^{*2} + a_2 I^* + a_3 = 0 \tag{37}$$

Where

$$a_1 = -(\mu+\delta_2+\alpha_1+\alpha_2)\beta_1\wp$$

$$a_2 = A\beta_2\wp - N(\mu+\delta_2+\alpha_1+\alpha_2)(\mu\wp+\delta_2\kappa\frac{\beta_1}{N}+\beta_2\wp)$$

$$a_3 = (\mu+\delta_2+\alpha_1+\alpha_2)\mu N\delta_2\kappa[R_0-1]$$

Let the following theorem analysis the local stability of the disease present equilibrium:

Theorem 3.

The Cholera disease present equilibrium E_{eq}^* is locally asymptotically stable if $R_0 > 1$ and unstable if $R_0 \leq 1$

Proof. When present $E_{eq}^* = (S^*; B^*; I^*)$ as the Cholera disease the present equilibrium of system (18) and the disease exists ($S^* \neq 0$, $I^* \neq 0$ *and* $B^* \neq 0$).

The Jacobian matrix at E_{eq}^* is given by:

(38)

$$J(E_{eq}^*) = \begin{pmatrix} -\mu-\beta_1\frac{I^*}{N}-\beta_2\frac{B^*}{\kappa+B^*} & -\beta_1\frac{S^*}{N} & -\beta_2\frac{S^*(\kappa+B^*)-SB^*}{(\kappa+B^*)^2} \\ \beta_1\frac{I^*}{N}+\beta_2\frac{B^*}{\kappa+B^*} & \beta_1\frac{S^*}{N}-(\mu+\delta_1)-(\alpha_1+\alpha_2) & \beta_2\frac{S^*(\kappa+B^*)-SB^*}{(\kappa+B^*)^2} \\ 0 & \wp & -\delta_2 \end{pmatrix}$$

. We see that the characteristic equation $\varphi(\lambda)$ of $J(E_{eq}^*)$ is:

$$\varphi(\lambda) = \lambda^3 + a_3\lambda^2 + a_2\lambda + a_1 \tag{39}$$

where

$$a_3 = (\mu + \beta_1 \tfrac{I^*}{N} + \beta_2 \tfrac{B^*}{\kappa+B^*}) + (\mu + \delta_1 + \alpha_1 + \alpha_2) + \delta_2 \tag{40}$$

$$\begin{aligned} a_2 = {} & (\mu + \beta_1 \tfrac{I^*}{N} + \beta_2 \tfrac{B^*}{\kappa+B^*})(\mu + \delta_1 + \alpha_1 + \alpha_2) + (\mu + \beta_1 \tfrac{I^*}{N} \\ & + \beta_2 \tfrac{B^*}{\kappa+B^*})\delta_2 + (\mu + \delta_1 + \alpha_1 + \alpha_2)\delta_2 - \beta_1 \tfrac{S^*}{N}(\beta_1 \tfrac{I^*}{N} \\ & + \beta_2 \tfrac{B^*}{\kappa+B^*}) - \wp\beta_2 \tfrac{S^*(\kappa+B^*) - SB^*}{(\kappa+B^*)^2}. \end{aligned} \tag{41}$$

$$a_1 = -\delta_2[(\mu + \beta_1 \tfrac{I^*}{N} + \beta_2 \tfrac{B^*}{\kappa+B^*})(\mu + \delta_1 + \alpha_1 + \alpha_2) - \beta_1 \tfrac{S^*}{N}(\beta_1 \tfrac{I^*}{N} + \beta_2 \tfrac{B^*}{\kappa+B^*})] - \wp\beta_2 \tfrac{S^*(\kappa+B^*) - SB^*}{(\kappa+B^*)^2}. \tag{42}$$

By routh- Hurwitz Criterion, the system (21) is locally asymptotically stable if $a_1 > 0$, $a2 > 0$ $a_3 > 0$ and $a_1 a_2 > a_3$.

Thus, the present equilibrium E^*_{eq} of system (21) is locally asymptotically stable if $R_0 > 1$.

4. Global Stability

4.1. The global stability of a disease-free cholera equilibrium. .

To show that the system (18) is globally asymptotically stable, we use the Lyapunov function theory for both the Cholera disease free equilibrium and the Cholera disease present equilibrium. First, we present the global stability of the Cholera disease-free equilibrium E^0_{eq}

Theorem 4. The Cholera disease free equilibruim E^0_{eq} is globally asymptotically stable Ω If $R_0 \leq 1$ and unstable otherwise.

Proof. Let the following Lyapunov function:

$$V : \Gamma \to \Re$$

$$V(S,I,B) = (S - S * ln\tfrac{S}{S^*}) + \tfrac{1}{\beta_1} I + \tfrac{1}{\delta_2} B, \tag{43}$$

$$\Gamma = \{(S,I,B) \in \Gamma / S > 0, I > 0, B > 0\}$$

(44)

$$\frac{dV}{dt} = -\frac{(\mu S-A)^2}{\mu S} - (1-\frac{A}{\mu S})(\frac{\beta_1 SI}{N} + \beta_2 \frac{SB}{\kappa+B}) + \frac{1}{\beta_1}(\beta_1 \frac{SI}{N} - I(\mu+\delta_1+\alpha_1+\alpha_2) + \beta_2 \frac{SB}{\kappa+B}) + \frac{1}{\delta_2}(\wp I - \delta_2 B).$$

Thus:

$$\frac{dV(S,I,B)}{dt} \leq 0$$

for $R_0 \leq 1$

Note do $\frac{dV}{dt} = 0$ if and only if $S = S_0$,$I = 0$ and $B = 0$.Hence, by Lasalle's invariance principle [16], E^0_{eq} is globally asymptotically stable in Γ.

4.2. Global stability of the Cholera disease present equilibrium. The final result of the global stability of E^*_{eq} in this section is as follows:

Theorem 5. The disease of Cholera disease present equilibrium point E^*_{eq} is globally asymptotically stable if $R_0 > 1$:

Proof. Let the Lyapunov function V:

$$V : \Gamma \to \Re$$

(45)
$$V(S,I,B) = S - S^* \ln\left(\frac{S}{S^*}\right) + I - I^* \ln\ln\left(\frac{I}{I^*}\right) + B - B^* \ln\left(\frac{B}{B^*}\right).$$

$$\Gamma = \{(S,I,B) \in \Gamma / S > 0, I > 0, B > 0\}$$

Then, the time derivative of the Lyapunov function is

(46)
$$\begin{aligned} \frac{dV}{dt} &= \left(1 - ln\left(\frac{S}{S^*}\right)\right)\left(A - \mu S - \beta_1 \frac{SI}{N} - -\beta_2 \frac{SB}{\kappa+B}\right) \\ &+ \left(1 - ln\left(\frac{I}{I^*}\right)\right)\left(\beta_1 \frac{SI}{N} - I(\mu+\delta_1+\alpha_1+\alpha_2) + \beta_2 \frac{SB}{\kappa+B}\right) + \left(1 - ln\left(\frac{B}{B^*}\right)\right)(\wp I - \delta_2 B). \end{aligned}$$

Then

$$\frac{dV(S,I,B)}{dt} \leq 0$$

Also ,we obtain $\frac{dV(S,I,B)}{dt} = 0 \Leftrightarrow I^* = I, B^* = B$ and $S^* = S$.

Hence, by LaSalle's invariance principle [16] the Cholera disease present equilibrium point E^*_{eq} is globally asymptotically stable on Γ.

5. SENSITIVITY ANALYSIS OF R_0 .

Sensitivity analysis is a powerful tool for evaluating how changes in parameter values influence the robustness of a model. It helps identify the key parameters that affect the basic reproduction number R_0, especially when considering assumptions about parameter values and uncertainties in data collection. Following the approach outlined by Chitnis et al. [10], we calculate the normalized forward sensitivity indices for R_0. Let

$$\mathrm{T}_u^{R_0} = \frac{\partial R_0}{\partial u} * \frac{u}{R_0} \tag{47}$$

Table 1 provides the sensitivity index of R_0 with respect to the parameter u.

Parameter	Description	Sensitivity indices
A	New populations are added to the model at a constant rate.	1.0000
μ	The natural death rate	1.0000
β_1	Transmission rate from human to human	1.0000
β_2	Transmission rate from environment to human	1.0000
α_1 ; α_2	Recovery rate from cholera	-1.5504
κ	Concentration of Vibrio cholera	-1.0000
δ_1	The death rate induced by the cholera	-0.1008
δ_2	Bacteria death rate	-0.9706
$\wp$	Shedding rate of bacteria by infectious population	1.0000

TABLE 1. Sensitivity indices of R_0

Table 1 shows that the threshold R_0 is directly sensitive to changes in the parameter values A, β_1, β_2, and $\wp$. This indicates that an increase or decrease in any of these parameters will result in a corresponding increase or decrease in R_0. Conversely, R_0 is inversely related to changes in μ, α_1, α_2, δ_1, and κ, meaning that a rise or fall in any of these parameters leads to a proportional decrease or increase in R_0.

6. NUMERICAL SIMULATIONS

In this section, we present numerical solutions to model (1) for various parameter values. To solve system (1), Gumel et al. [21] developed the Gauss-Sade-like implicit finite-difference

method (GSS1 method), as detailed in [22]. Main results.

The fundamental data values: The model's parameters are displayed in a table2. The sources are also cite.

Parameter	Baseline value	Reference
A	10	Assumed
μ	0.025	[24]
β_1	0.02	[23]
β_2	0.02	[23]
α_1 ; α_2	0.214	[24]
κ	$10^4 cell/day$	Assumed
δ_1	0.013	[25]
δ_2	0.33	[26]
$\wp$	10 cell/day	[25]

TABLE 2. Baseline Parameter values for system(21)

First, we graphically illustrate the cholera disease-free equilibrium E^0_{eq}, using the initial values and parameters listed in Table 2, where $R_0 < 1$.

By varying the initial values of the variables $S(0)$, $I(0)$, $C(0)$, and $R(0)$, the following observations were made:

- The susceptible population steadily increases and approaches $S(0) = 250$ (see Figure 2(a)).
- The number of patients in the treatment center decreases and approaches zero (see Figure 2(b)).
- The populations of carriers and symptomatic infected individuals initially rise but then decrease, nearing zero (see Figure 2(c)).
- The number of recovered individuals also declines, approaching zero (see Figure 2(d)).

These results show that the solution curves converge to the equilibrium $E^0_{eq} = (S_0, 0, 0, 0)$ when $R_0 < 1$. Thus, the model (1) is globally asymptotically stable.

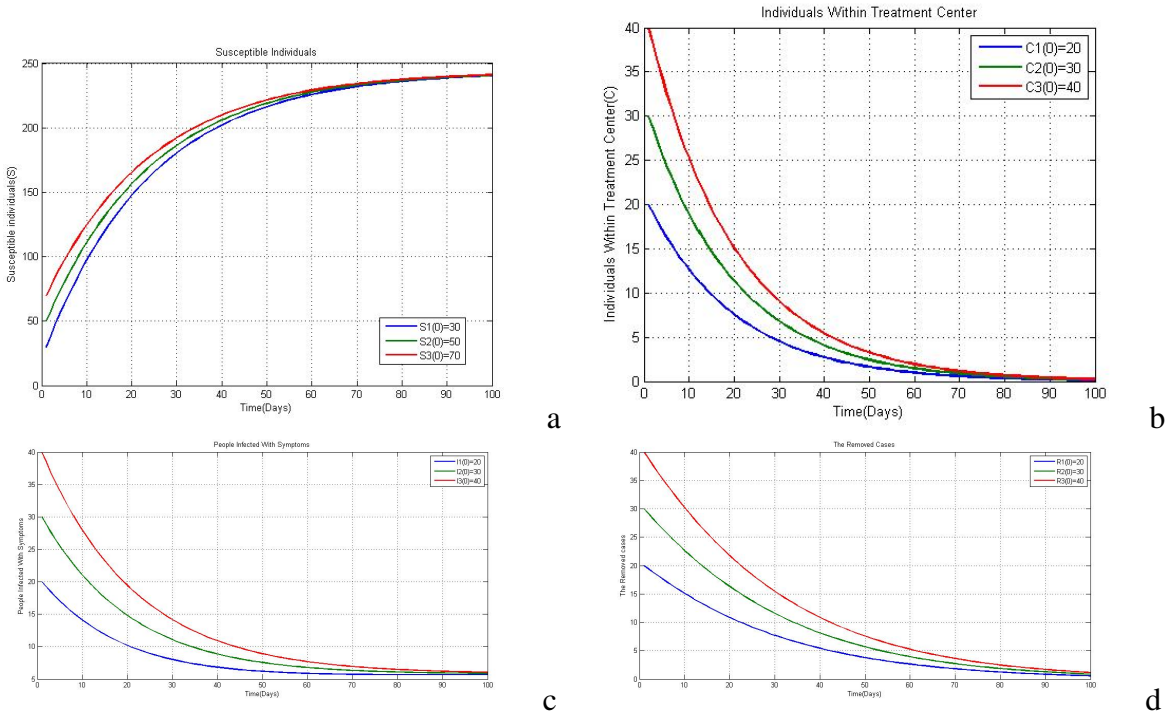

FIGURE 2.

We have identified an equilibrium for cholera when $R_0 > 1$. According to Theorem (5), the cholera disease equilibrium E^*_{eq} for system (1) is globally asymptotically stable.

To illustrate this, we provide a graphical representation of the cholera disease equilibrium E^*_{eq}, using the parameters and initial values specified in Table 2, where $R_0 > 1$.

The total number of susceptible individuals initially increases, then experiences a slight decline, ultimately approaching $S^* = 42$. The proportion of infected cases with no or only mild symptoms initially decreases rapidly before experiencing a slight rise (See Figure 3 (a)).Concerning the patient population at the treatment center is advancing towards the threshold of 16(Figure 3(b)).The number of carriers of the bacteria and symptomatic infected individuals converge at $I^* = 24$ (See Figure 3(c)). As the number of recovered individuals grows, it approaches the target value of $R^* = 170$ (See Figure 3(d)). This indicates that the recovery rate is improving and the number of individuals who have successfully recovered is nearing the desired threshold.

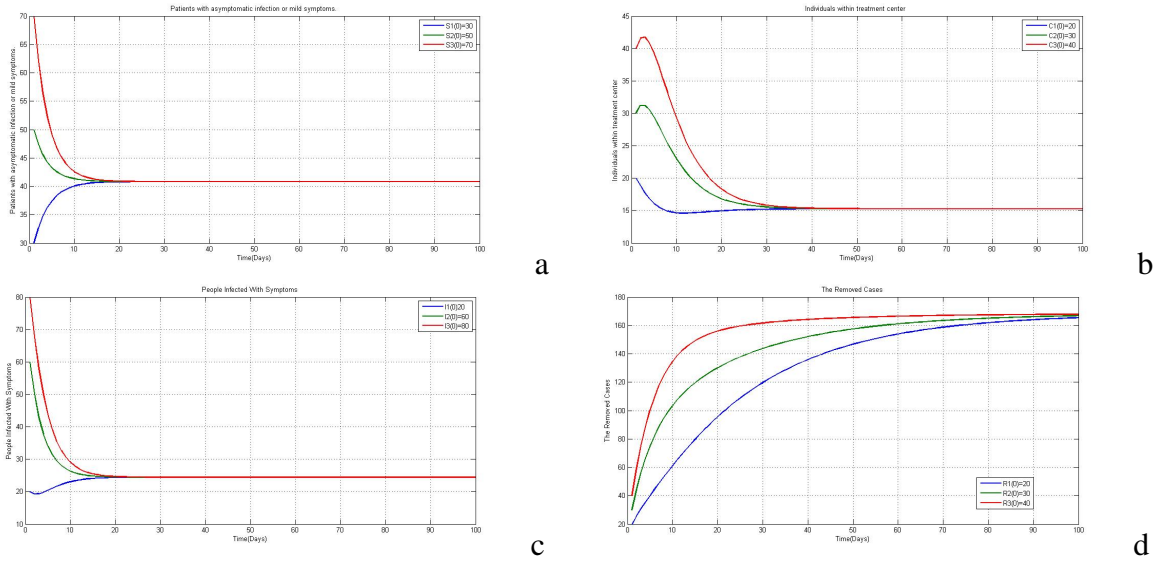

FIGURE 3.

7. CONCLUSION

In this study, we developed and presented a continuous SICR-B mathematical model to describe the dynamics of cholera transmission. We derived the basic reproduction number R_0 for the system as follows:

$$R_0 = \beta_1 \frac{A}{\mu N(\mu + \delta_1 + \alpha_1 + \alpha_2)} + \beta_2 \frac{A\wp}{\delta_2 \kappa \mu(\mu + \delta_1 + \alpha_1 + \alpha_2)}$$

This expression for R_0 provides insight into the system's behavior. We performed a sensitivity analysis on the model parameters to identify those that have a significant influence on the reproduction number R_0. Additionally, we applied stability analysis theory for nonlinear systems to assess both the local and global stability of the cholera model.

Our analysis indicates that the disease-free equilibrium E^0_{eq} is locally asymptotically stable when $R_0 \leq 1$, meaning that the disease will eventually be eradicated. On the other hand, if $R_0 > 1$, the endemic equilibrium E^*_{eq} becomes locally asymptotically stable, suggesting that the disease will persist in the population. Furthermore, by employing a Lyapunov function, we demonstrated that E^0_{eq} is globally asymptotically stable when $R_0 \leq 1$, and E^*_{eq} is globally asymptotically stable when $R_0 > 1$.

CONFLICT OF INTERESTS

The authors declare that there is no conflict of interests.

REFERENCES

[1] J.B. Kaper, J.G. Morris Jr, M.M. Levine, Cholera, Clin. Microbiol. Rev. 8 (1995), 48–86. https://doi.org/10.1128/cmr.8.1.48.

[2] C.T. Codeço, Endemic and epidemic dynamics of cholera: The role of the aquatic reservoir, BMC Infect Dis. 1 (2001), 1. https://doi.org/10.1186/1471-2334-1-1.

[3] D.L. Heymann, Control of communicable diseases manual, APHA Press, 2015.

[4] N. Ferguson, Capturing human behaviour, Nature 446 (2007), 733–733. https://doi.org/10.1038/446733a.

[5] E.J. Nelson, J.B. Harris, J. Glenn Morris Jr, S.B. Calderwood, A. Camilli, Cholera transmission: the host, pathogen and bacteriophage dynamic, Nat. Rev. Microbiol. 7 (2009), 693–702. https://doi.org/10.1038/nrmicro2204.

[6] S. Samanta, S. Rana, A. Sharma, A.K. Misra, J. Chattopadhyay, Effect of awareness programs by media on the epidemic outbreaks: A mathematical model, Appl. Math. Comp. 219 (2013), 6965–6977. https://doi.org/10.1016/j.amc.2013.01.009.

[7] R.P. Agarwal, Difference equations and inequalities: theory, methods, and applications, CRC Press, 2000.

[8] A. Mwasa, J.M. Tchuenche, Mathematical analysis of a cholera model with public health interventions, Biosystems 105 (2011), 190–200. https://doi.org/10.1016/j.biosystems.2011.04.001.

[9] E. Sebastian, P. Victor, Optimal control strategy of a discrete-time svir epidemic model with immigration of infectives, Int. J. Pure Appl. Math. 113 (2017), 55–63.

[10] N. Chitnis, J.M. Hyman, J.M. Cushing, Determining important parameters in the spread of malaria through the sensitivity analysis of a mathematical model, Bull. Math. Biol. 70 (2008), 1272–1296. https://doi.org/10.1007/s11538-008-9299-0.

[11] M. Tahir, S. Inayat Ali Shah, G. Zaman, S. Muhammad, Ebola virus epidemic disease its modeling and stability analysis required abstain strategies, Cogent Biol. 4 (2018), 1488511. https://doi.org/10.1080/23312025.2018.1488511.

[12] A.B. Gumel, P.N. Shivakumar, B.M. Sahai, A mathematical model for the dynamics of HIV-1 during the typical course of infection, Nonlinear Anal.: Theory Meth. Appl. 47 (2001), 1773–1783. https://doi.org/10.1016/s0362-546x(01)00309-1.

[13] A. Mwasa, J.M. Tchuenche, Mathematical analysis of a cholera model with public health interventions, Biosystems 105 (2011), 190–200. https://doi.org/10.1016/j.biosystems.2011.04.001.

[14] Z. Hu, Z. Teng, H. Jiang, Stability analysis in a class of discrete SIRS epidemic models, Nonlinear Anal.: Real World Appl. 13 (2012), 2017–2033. https://doi.org/10.1016/j.nonrwa.2011.12.024.

[15] M. Kot, Elements of mathematical ecology, Cambridge University Press, Cambridge, 2000.

[16] J.P. La Salle, The stability of dynamical systems, SIAM, 1976.

[17] P.N. Okolo, A.S. Magaji, I. Joshua, P.F. Useini, Mathematical modelling and analysis of cholera disease dynamics with control, Fudma J. Sci. 4 (2021), 363–381. https://doi.org/10.33003/fjs-2020-0404-494.

[18] A. Bouaine, M. Rachik, K. Hattaf, Optimization strategies are applied to discrete epidemic models with specific nonlinear incidence rates, Int. J. Math. Appl. 4 (2016), 73–80.

[19] P. van den Driessche, J. Watmough, Reproduction numbers and sub-threshold endemic equilibria for compartmental models of disease transmission, Math. Biosci. 180 (2002), 29–48. https://doi.org/10.1016/s0025-5564(02)00108-6.

[20] M. Bani-Yaghoub, R. Gautam, Z. Shuai, P. van den Driessche, R. Ivanek, Reproduction numbers for infections with free-living pathogens growing in the environment, J. Biol. Dyn. 6 (2012), 923–940. https://doi.org/10.1080/17513758.2012.693206.

[21] A.B. Gumel, P.N. Shivakumar, B.M. Sahai, A mathematical model for the dynamics of HIV-1 during the typical course of infection, Nonlinear Anal.: Theory Meth. Appl. 47 (2001), 1773–1783. https://doi.org/10.1016/s0362-546x(01)00309-1.

[22] J. Karrakchou, M. Rachik, S. Gourari, Optimal control and infectiology: Application to an HIV/AIDS model, Appl. Math. Comp. 177 (2006), 807–818. https://doi.org/10.1016/j.amc.2005.11.092.

[23] T.W. Hartley, Public perception and participation in water reuse, Desalination 187 (2006), 115–126. https://doi.org/10.1016/j.desal.2005.04.072.

[24] A.J. Falaye, F. Awonusi, O. Eseyin, et al. The weak form market efficiency and the Nigerian stock exchange, Afro Asian J. Soc. Sci. 9 (2018), 1–17.

[25] J. Wang, C. Modnak, Modeling cholera dynamics with controls, Canad. Appl. Math. Quart. 19 (2011), 255–273.

[26] P. Kumar, D.K. Mishra, D.G. Deshmukh, et al. Vibrio cholerae O1 Ogawa El Tor strains with the ctxB7 allele driving cholera outbreaks in south-western India in 2012, Infect. Genetics Evol. 25 (2014), 93–96. https://doi.org/10.1016/j.meegid.2014.03.020.